

Edge Plasma Analysis for Liquid-Wall MFE Concepts*

R. W. Moir, M. Rensink, and T. D. Rognlien

University of California Lawrence Livermore National Laboratory
Livermore, CA, 94551 USA

e-mail Moir1@LLNL.GOV

Abstract. A thick flowing layer of liquid (e.g., flibe—a molten salt, or $\text{Sn}_{80}\text{Li}_{20}$ —a liquid metal) protects the structural walls of the magnetic fusion configuration so that they can last the life of the plant even with intense 14 MeV neutron bombardment from the D-T fusion reaction. The surface temperature of the liquid rises as it passes from the inlet nozzles to the exit nozzles due to absorption of line and bremsstrahlung radiation, and neutrons. The surface temperature can be reduced by enhanced turbulent convection of hot surface liquid into the cooler interior. This surface temperature is affected by the temperature of liquid from a heat transport and energy recovery system. The evaporative flux from the wall driven by the surface temperature must also result in an acceptable impurity level in the core plasma. The shielding of the core by the edge plasma is modeled with a 2D-transport code for the DT and impurity ions; these impurity ions are either swept out to the divertor, or diffuse to the hot plasma core. An auxiliary plasma between the edge plasma and the liquid wall may further attenuate evaporating flux of atoms and molecules by ionization near the wall.

1. Introduction

Walls of liquid lithium or molten salt have long been recognized as a solution to the first-wall problem if a plasma of fusion quality can be operated in their presence [1]. Development of a workable design would result in a paradigm shift for power-plant concepts, including greatly reduced wall damage, higher neutron wall loading by up to an order of magnitude, and reduced cost of electricity by more than 35% [2-3]. A development strategy shows large cost savings if liquid walls are demonstrated to be viable, consistent with a lower-cost materials development program. A wider choice of structural materials also becomes available. In addition, liquid divertors may allow highly localized heat flux.

Two major topics related to the use of liquid walls are addressed in this paper: (1), reduction of the surface temperature to keep evaporation low; and (2), determination of the maximum evaporative flux that the DT edge plasma can adequately shield the core from impurity contamination. For molten salt (flibe, Li_2BeF_4), one can reduce surface temperature by inducing convection from small droplets sprayed onto the surface, which enhances thermal conductivity. For liquid metals (e.g., $\text{Sn}_{80}\text{Li}_{20}$), laminar thermal conductivity is higher but more difficult to enhance. Also, liquid metal flow paths must be virtually identical with magnetic field lines. The core impurity concentration is predicted using detailed transport simulations of impurity ions through the edge plasma, thus determining the maximum allowable evaporative flux[4] and hence surface temperature.

We are studying three configurations: tokamak, spheromak and field reversed configuration (FRC). The tokamak is shown in Fig. 1. The other two configurations are the spheromak (Fig. 2) and the FRC (Fig. 3). In both these configurations, unlike the tokamak, the liquid flow is nearly aligned with the magnetic field thus permitting the use of liquid metals in addition to flibe. The FRC edge plasma flows to a distant end tank where gas influx from recycling is assumed small. Spheromak characteristics are between the tokamak and FRC.

2. Heat transfer model, effective surface temperature, and evaporative flux

The surface temperature is calculated for a given heat load using the heat transfer characteristics of the liquid. A surface fluid element is followed from the time it leaves a nozzle till it enters an exit nozzle. The factor $(F+1)$ represents the enhancement of heat conduction due to turbulent eddy motion; $F = 0$ gives the laminar case. Magnetic

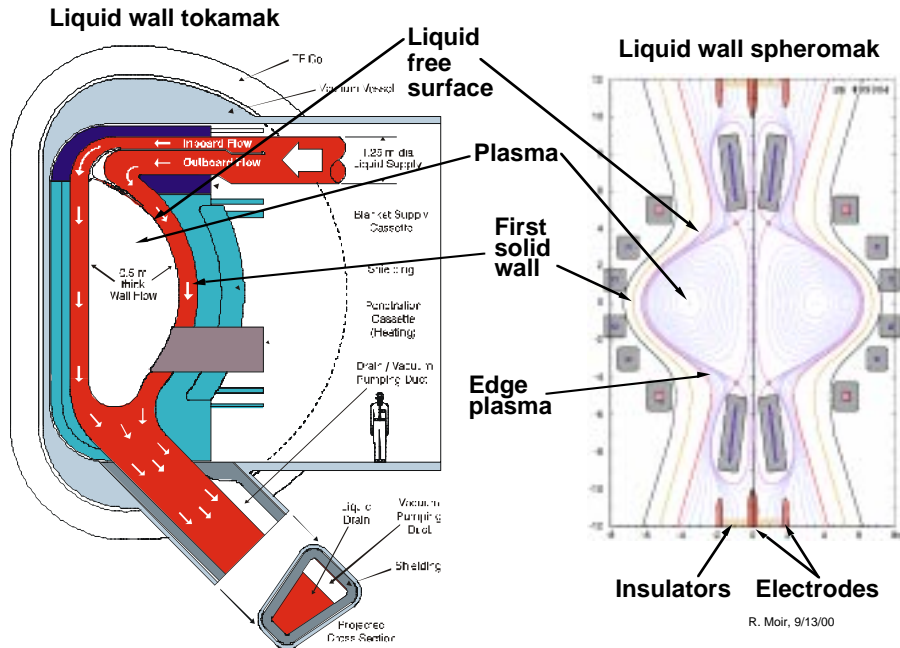


Fig. 1. Tokamak with a thick liquid wall.

Fig. 2. Spheromak with a thick liquid wall.

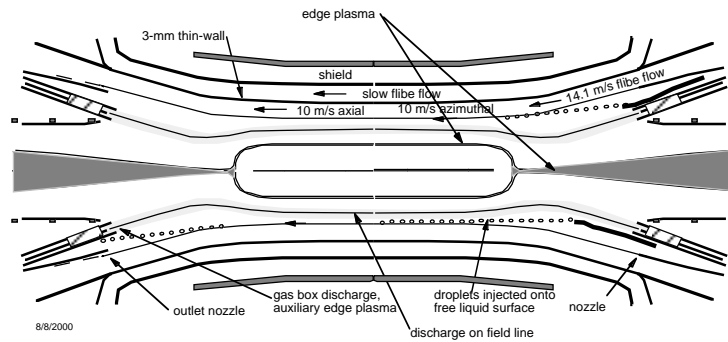


Fig. 3. FRC with a thick liquid wall

fields will tend to laminarize the flow, reducing F . Here F is treated as a parameter; however, theoretical work by Smolentsev[5] and his planned experiments should improve the predicted value of F . One idea to produce enhanced mixing (large F values) is to spray droplets onto the surface. They must be small enough not to cause splashing and large enough to cause persistent vortex motion. Another idea is to use structures within the flow to induce vortices. Figure 4 gives the wall temperature for flibe and SnLi subjected to 1 MW/m^2 for various F values.

The wall temperature determines the evaporative flux for the edge plasma calculations. Evaporative flux, J , into a vacuum is determined by the relations

$$J = \frac{n\bar{v}}{4}, \quad \bar{v} = \sqrt{\frac{8kT}{\pi m}}, \quad n = \frac{P}{kT} \quad \Rightarrow \quad J = \frac{P}{\sqrt{2\pi mkT}}. \quad (1)$$

The density, n , is that present at equilibrium when evaporation equals condensation. The evaporative flux of the various liquids is plotted in Fig. 5. Because the flux is a very nonlinear function of temperature, one needs to average the flux along the wall, which can be parameterized by the temperature T_{eff} , with $T_{\text{eff}} > T_{\text{ave}}$.

3. Edge-plasma characteristics and impurity shielding

The plasma in the edge region is modeled by the two-dimensional plasma transport code UEDGE, which evolves equations for the plasma density, parallel ion velocity, separate

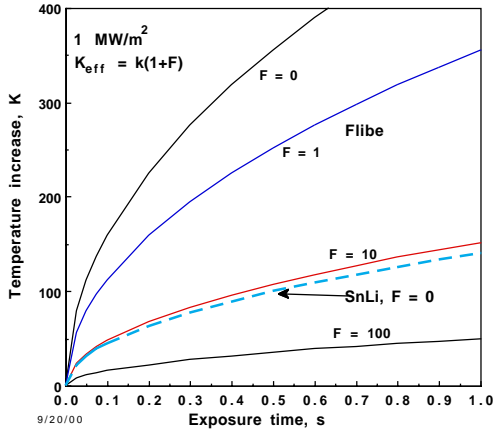


Fig. 4. Temperature rise of the fluid element versus time at 1.0 MW/m^2 .

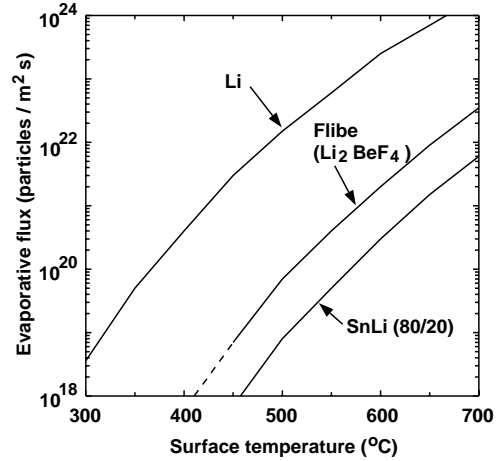


Fig. 5. Evaporative flux into vacuum for candidate liquids.

electron and ion temperatures, and neutral gas density [6]. The code follows a DT fuel species, and each charge state of the impurity ions from vapor emitted at the liquid sidewall. Parallel transport along the B-field is taken as classical, while cross-field diffusion is assumed enhanced to $0.33 \text{ m}^2/\text{s}$ for density and $0.5 \text{ m}^2/\text{s}$ for energy by plasma turbulence. There are three important differences between a tokamak and FRC: (1), the magnetic connection length along the B-field from the midplane to the effective end of the device (null-point region) is $\sim 4 \text{ m}$ for the FRC, much shorter than for a tokamak which has a strong toroidal magnetic field; (2), the FRC is low recycling while the tokamak can be either high or low recycling; and (3), the power density from the FRC is much larger, so more energy flux is available to ionize impurities.

3.1 FRC edge plasma

A slab model is used to approximate the thin annular scrape-off layer (SOL) region beyond the magnetic separatrix. In the axial direction, the SOL plasma contacts the core boundary along an 8-m length, followed by a 2 m exit region. The radial domain begins at the separatrix at 0.39 m and extends radially for 2.5 cm; the vapor gas source flows in from this outer boundary for computational efficiency. The results are not sensitive to the outer boundary location other than determining the effective gas flux in the converging cylindrical geometry, which needs more study. The input parameters for the core plasma edge boundary are taken from Table 1 of Ref.[8]. The edge density is assumed to be $2 \times 10^{20} / \text{m}^3$ or 0.1 of the core density. The energy flux is 20 MW/m^2 , split equally between ions and electrons. The calculated radial decay length for the DT fuel density is then 0.38 cm. The separatrix temperatures are $T_e = 1.44 \text{ keV}$ and $T_i = 1.50 \text{ keV}$. The radial decay lengths for Te and Ti are 0.43 cm and 0.60 cm, respectively.

The impurity gas is injected as a uniform flux from the sidewall since tests with nonuniform injection show little change in the results. The calculated impurity density on the separatrix at the midplane versus gas flux is shown in Fig. 6 for lithium (Li) from SnLi and for fluorine (F) from flibe. Note that fluorine penetrates to the core boundary more easily than lithium, as in the tokamak case [7], due, in part, to its higher ionization potential.

The tolerable amount of impurities in the core can be set by DT fuel dilution or radiation loss. For impurities with low to moderate maximum charge state Z , dilution is the main concern. The fractional fusion power reduction from dilution is $2Z n_z / n_{\text{DT}}$, where n_z and n_{DT} are the impurity and DT fuel densities, respectively [7]. Thus, a 20% power reduction for Li ($Z=3$) and F ($Z=9$), sets concentration limits of 0.03 and 0.01, respectively. Since the concentration levels of relevance are deep within the core, one can either assume that the core impurity density is flat with the same value as at the edge, or that the impurity and DT densities vary

together in the core such that the concentration remains a constant. These two assumptions give two limits to the operating points in Fig.6, labeled (for F) 1% edge and 1% core. An argument for choosing the flat density case (1% core) is that the source of impurities is on the outside, but more detailed core analysis needs to be done.

The maximum allowable edge impurity densities shown in Fig. 6 give the corresponding gas flux limits from the wall, and using Fig. 5, yield the temperature limits. These gas fluxes can then be plotted on curves of wall temperature versus evaporative flux as shown in Fig. 7. These points thus identify the allowable wall temperature to prevent excessive impurity intrusion into the core plasma. For the FRC, core impurity limits require T_{eff} between 560 and 630 °C for flibe and between 660 and 720 °C for SnLi. However, heat transport and recovery analysis give estimates of $T_{\text{eff}} = 660$ for flibe and 715 °C for SnLi[8]. Thus, flibe evaporation is a factor of ten too high, but SnLi is acceptable.

3.2 Tokamak edge plasma

Similar calculations with UEDGE code for the tokamak were reported in [7]. Here the parallel loss distance along \mathbf{B} is 80 m compared to 4 m for the FRC. The DT edge density is $2 \times 10^{19} \text{ m}^{-3}$ for low recycling and $4 \times 10^{19} \text{ m}^{-3}$ for high recycling. The impurity edge density versus flux is shown in Fig. 8a and 8b, and the allowed temperature limits are plotted in Fig. 9. For low recycle plasmas with Li, operation is allowed at $T_{\text{eff}} = 375$ °C (not shown). If thermal conversion efficiency requires the inlet temperature to be 325 °C and the outlet temperature 475 °C [9], giving $T_{\text{eff}} \approx 440$ °C, then Li evaporation is about ten times too much. For high recycle plasmas (all but Li divertors), for SnLi core contamination restricts T_{eff} to 475 °C. but T_{eff} is predicted to be 610 °C (inlet 400 and outlet of 725 °C) from heat transfer considerations[9]. Thus, SnLi evaporation is about ~100 too much. Flibe core contamination restricts T_{eff} below 400 °C whereas thermal conversion gives at least 540 °C [9]. Consequently, to make flibe practical we need to reduce evaporation by ~1000.

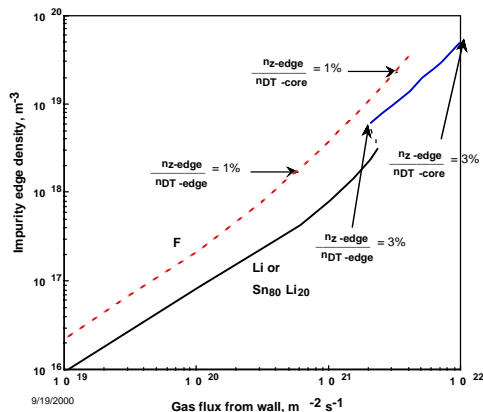


Fig. 6. Plot of impurity edge density vs average evaporative flux for FRC.

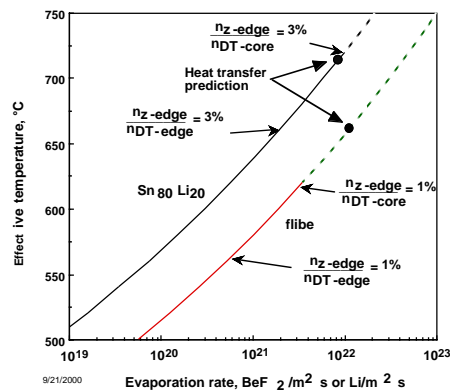
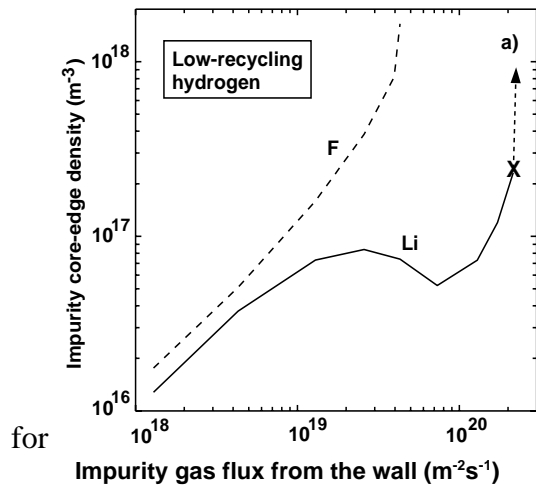


Fig. 7. Effective surface temperature of the FRC versus evaporative flux showing allowed temperature points.

4 Conclusions

The crucial issue of the evaporating liquid overly contaminating the core plasma has been addressed for Li, SnLi, and flibe. For the FRC, liquid wall hydraulics and contamination appear acceptable for SnLi. Additional study is needed for auxiliary shielding plasmas and strong enhancement of heat transfer near the free liquid surface for flibe. For the tokamak, we



for

Impurity gas flux from the wall ($\text{m}^{-2}\text{s}^{-1}$)

Fig. 8a. Edge impurity vs flux for low recycle tokamak.

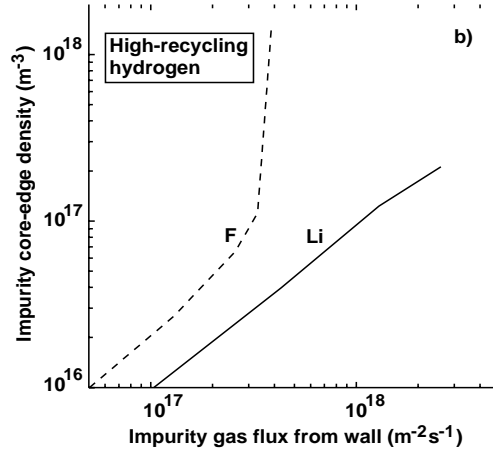


Fig. 8b. Edge impurity vs flux for high recycle.

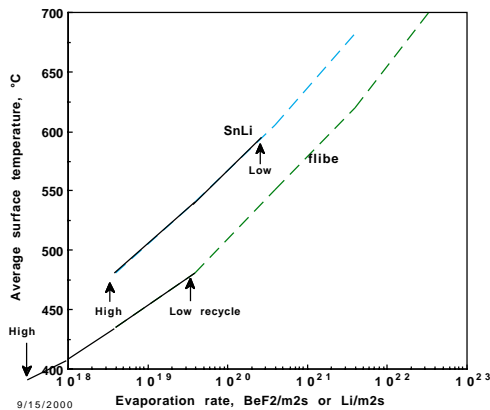


Fig. 9. Average surface temperature versus evaporation rate where UEDGE says the core plasma is not overly contaminated with impurities. The dashed lines show where evaporation must be reduced by for example auxiliary edge plasma heating.

need innovative solutions to a number of problems such as too much evaporation by a factor of 10 design problems. For the spheromak, we need some but not all of the tokamak solutions. Liquids other than those considered here, including non-lithium-containing liquids, may give optimum performance. We are encouraged to carry out further work in this promising area of liquid wall protection for fusion power plant design.

5 Acknowledgements. *Work performed under the auspice of the U.S. Department of Energy by University of California Lawrence Livermore National Laboratory under Contract W-7405-Eng-48.

6 References

- [1] CHRISTOFILOS, N.C., J. Fusion Energy **8** (1989) 97.
- [2] MOIR, R.W., Nucl. Fusion **37** (1997) 557.
- [3] MOIR, R.W., Comments on Plasma Physics and Controlled Fusion, **2** (2000) 99-111.
- [4] MOIR, R.W., RENSINK, M.E., and ROGNLIEN, T.D., et al., contributing authors, APEX Interim Report, UCLA-ENG-99-209 (1999), Chapters 5 and 12. ABDU, M., et al., Fusion Eng Design, in press (2000).
- [5] SMOLENTSEV, S., et al., submitted to Int J. Heat Mass Transfer (2000).
- [6] ROGNLIEN, T. D., et al., Contr. Plasma Phys., **34** (1994) 362.
- [7] ROGNLIEN, T. D. and RENSINK, M, J. Nucl. Mater., to be pub., (2000).
- [8] MOIR, R. W., et al., 13th ANS Topical mtg tech fusion energy, Oct, 2000, Park City, Utah, UCRL-JC-139086 Abs.
- [9] MORLEY, N., UCLA, private communications, September, 2000.